Multiplexing technique using amplitude-modulated chirped fibre Bragg gratings with applications in two-parameter sensing

Author:
Wong, Allan; Childs, Paul; Peng, Gang-Ding

Publication details:
Photonics Asia 2007: Sensors and Imaging

Event details:
Photonics Asia 2007: Sensors and Imaging
Beijing, China

Publication Date:
2007

Publisher DOI:
http://dx.doi.org/10.1117/12.754678

Multiplexing technique using amplitude-modulated chirped fibre Bragg gratings with applications in two-parameter sensing

Allan C. L. Wong, Paul A. Childs and Gang-Ding Peng*
School of Electrical Engineering and Telecommunications,
University of New South Wales, Sydney, NSW 2052, Australia
*Corresponding author. E-mail: g.peng@unsw.edu.au; Ph: +61-2-93854014

ABSTRACT

A multiplexing technique using amplitude-modulated chirped fibre Bragg gratings (AMCFBGs) is presented. This technique realises the multiplexing of spectrally-overlapped AMCFBGs with identical centre Bragg wavelength and bandwidth. Since it is fully compatible with the wavelength division multiplexing scheme, the number of gratings that can be multiplexed can be increased by several times. The discrete wavelet transform is used to demodulate such multiplexed signal. A wavelet denoising technique is applied to the multiplexed signal in conjunction with the demodulation. Strain measurements are performed to experimentally demonstrate the feasibility of this multiplexing technique. The absolute error and crosstalk are measured. An application to simultaneous two-parameter sensing is also demonstrated.

KEYWORDS: Amplitude-modulated chirped fibre Bragg grating, Spectral-overlap multiplexing, Discrete wavelet transform, Strain, Temperature, Two-parameter sensing.

1. INTRODUCTION

Fibre Bragg gratings (FBGs) have been used extensively as fibre-optic sensors due to their superior properties, such as the unique wavelength-encoded characteristics; immunity to electromagnetic interference and moist conditions; ease of multiplexing along a single optical fibre; high strain resolution and measurement range; resistance to corrosion; high temperature capacity; long lifetime; small and compact size; and the ability to be installed by embedding or surface-mounting [1 – 3]. In sensing, a definite advantage of using fibre-optic sensors is their ability of quasi-distributed (multipoint) sensing through multiplexing, which is one of the building blocks of a robust and cost effective sensor system. There are a wide variety of multiplexing schemes being developed and proposed, among which the wavelength division multiplexing (WDM) is the most widely used scheme for FBGs [3 – 5].

Chirped FBGs (CFBGs), when being used as sensors, behave similarly to uniform FBGs. So, CFBGs can be used in applications where uniform FBGs are employed. Additionally, chirped FBGs offer advantages in certain applications, such as the detection of cracking, and distributed profile measurement of strain, temperature and wear of a structure [6 – 11]. However, one of the main issues of using CFBGs is that the number of gratings that can be multiplexed is limited when using WDM, because of the large spectral bandwidth each chirped FBG occupies within the light source spectrum without overlapping. In this paper, this issue is addressed by a sensor system with a special type of grating called the amplitude-modulated CFBGs (AMCFBGs). Each AMCFBG is fabricated such that a unique amplitude modulation appears on the flat-top region of its reflection spectrum. As such, even when the gratings are completely overlapped with similar spectral characteristics, they can still be uniquely identified using some signal processing techniques. In this case, the discrete wavelet transform (DWT) is used to demultiplex and demodulate the multiplexed sensor signal. Noise reduction is performed concurrently with the DWT demodulation through a wavelet denoising technique. With these unique amplitude modulations, the gratings are said to be multiplexed via the spectral-overlap multiplexing scheme; and the number of gratings that can be multiplexed is increased by several times when used in conjunction with the WDM scheme. In this paper, a multiplexing technique using the spectrally-overlapped AMCFBGs is presented. The

Advanced Sensor Systems and Applications III, edited by Yun-Jiang Rao, Yanbiao Liao,
Gang-Ding Peng, Proc. of SPIE Vol. 6830, 683010, (2007)
0277-786X/07/$18 · doi: 10.1117/12.754678

performance of the sensor system, in terms of the resolution, accuracy and crosstalk, are investigated through strain measurements. The application of this multiplexing technique is demonstrated through the simultaneous measurement of strain and temperature of a metal alloy plate.

2. MULTIPLEXING PRINCIPLE

2.1 Principle of spectral-overlap multiplexing

The principle of this spectral-overlap multiplexing technique is briefly described here, followed by more detailed discussions. The AMCFBGs are fabricated with unique signatures – sinusoidal amplitude modulations of different frequencies. Having a unique signature for each AMCFBG, they can be multiplexed via the spectral-overlap multiplexing by simply 'stacking' the gratings with similar spectral characteristics, namely the centre Bragg wavelength and bandwidth. Since the spectral-overlap multiplexing is fully compatible with the WDM scheme, other sets of AMCFBGs having different centre Bragg wavelengths may be added to form a sensor network. With an interrogation and data acquisition system, the measurand-induced wavelength shift of the sensor signal can be obtained. The multiplexed signal is then demultiplexed and demodulated using the DWT demodulation. Concurrently, a wavelet denoising technique called the block-level-thresholding (BLT) is applied to reduce the noise associated with the sensor signal. By taking the DWT, the sensor signal is decomposed into detail and approximation coefficients. The higher levels of detail coefficients are used to extract the unique signatures of the AMCFBGs, with one signature of AMCFBG appears on one wavelet level. At the same time, the lower levels of detail coefficients, predominately consist of noise, are readily discarded through the BLT, and so the noise components are effectively removed. Finally, the measurand-induced wavelength shift of the sensor signal can be tracked by measuring the 'phase-shift' of the unique signatures, the the final measurand outputs can then be determined.

2.2 Fabrication of AMCFBGs

The fabrication of an AMCFBG is similar to that of an apodised, unchirped FBG, so a standard FBG-writing facility and linear chirped phase masks that are commercially available should be able to fabricate these specially tailored gratings. The subtle difference is the addition of an amplitude-modulation function to the refractive index modulation of the core of a fibre, which can be achieved by varying the induced DC refractive index during the writing process. With this index modulation, the reflection spectrum has a unique signature – a sinusoidal modulation on the flat-top region. The amplitude-modulation function for the refractive index modulation along the axial direction of the fibre, z, is given by,

$$f_v(z) = w \cdot \sin^2(\pi v z / L), \tag{1}$$

where w is an apodisation function such as a raised-cosine function, v is the frequency (i.e., the number of periods per unit bandwidth) of modulation, and L is the length of the grating. The reflection spectrum for one AMCFBG can be approximated by the expression,

$$R(\lambda) \approx \chi_{(\lambda_{\min}, \lambda_{\min} + c_L L)}(\lambda)\left[R_{\min} + (R_{\max} - R_{\min}) f_d\left(\frac{\lambda - \lambda_{\min}}{c_L} \right) \right], \tag{2}$$

where λ_{min} is the initial wavelength of the grating, R_{min} and R_{max} are the reflectivities of the troughs and peaks of the grating spectrum, respectively, c_L is the linear chirp rate of the phase mask used for writing the gratings, and $\chi_I(x)$ is the characteristic function on the interval I which equals 1 when x is an element of I and zero otherwise.

2.3 Spectral-overlap Multiplexing of AMCFBGs

There have been many methods proposed previously that utilise the spectral-overlap multiplexing, such as carrier modulation [12, 13], intensity modulation [14], optical coherence function [15], minimum variance shift using genetic algorithm [16, 17], and the use of chirped FBG based Fabry-Perot cavity sensors [18]. In the present multiplexing technique, an important criterion is to have some mechanisms to uniquely identify each spectrally overlapped AMCFBG; otherwise, they will not be able to distinguish one from another. The uniqueness of each AMCFBG is defined by the frequency of its amplitude-modulation; with the condition that for a set of overlapped gratings with the same centre Bragg wavelength, no two gratings can have the same modulation frequency. By combining the spectral-overlap multiplexing with the WDM scheme, the maximum number of AMCFBGs that can be multiplexed is the number of gratings that are spectrally overlapped with the same centre Bragg wavelength, times the number of gratings in the WDM arrangement. It is noted that the number of gratings that can be overlapped depends largely on the number of periods of

sinusoidal modulations that can be fabricated with good quality and fringe visibility. This in turn depends on the fabrication technique and the availability of equipment. Currently, gratings with amplitude modulations of nine periods have been fabricated in our facility with moderate quality and fringe visibility. This can be improved if better fabrication techniques and/or more sophisticated equipment are used.

2.4 Demodulation of AMCFBGs

The second important criterion for the spectral-overlap multiplexing is to have a viable method to demultiplex and demodulate the multiplexed (and overlapped) signal, and that can be accomplished by using the DWT demodulation. The principle of this demodulation is described in [19]. An AMCFBG signal can be represented by a wavelet series of different levels $j = 1,2,...,J$, i.e.,

$$R(\lambda) = \sum_m A_J + \sum_m \sum_{j=1}^{J} D_j \ , \tag{3}$$

where $j, m \in Z$. A_j and D_j are the approximation and detail parts of the signal that consist of lower half and higher half of frequency components of the whole signal bandwidth, respectively. The frequency of the signal decreases with increasing wavelet levels. Since the frequencies of the sinusoidal modulations are very low, they naturally appear in higher wavelet levels. The modulation of each grating can be distinctly identified in one of those high wavelet levels, and the measurand-induced wavelength shift can be tracked by measuring the 'phase-shift' of the sinusoidal modulation. Concurrently, the BLT denoising technique [19] is applied with the DWT demodulation, removing all the wavelet coefficients at levels lower than the wavelet level of interest. Since almost all of the noise components appear in the lower wavelet levels, they are effectively removed, and so the demodulated signal is very much noise free. As the demultiplexing and demodulation of the overlapped AMCFBGs are carried out digitally by computer programs, no complicated demodulating electronics are needed, thus reducing the complexity of the sensor system.

3. EXPERIMENTAL INVESTIGATION OF SENSOR SYSTEM PERFORMANCE

3.1 Experimental setup

The performance of the multiplexing technique using AMCFBGs is investigated through strain measurements. The experimental setup is shown in Fig. 1. A tuneable laser source was launched into four AMCFBGs via a 3 dB fibre-optic coupler. The AMCFBGs were fabricated using two chirped phase masks, both with a linear chirp-rate of 1.32 nm/mm. Sinusoidal modulations with apodisation were achieved by dithering the phase mask according to the modulation function as the laser beam scanned across it. One set of gratings, S1 and S2, was written with a centre Bragg wavelength of 1530 nm, a bandwidth of ~15 nm and amplitude modulations of 3 and 5 periods. The reflection spectra are shown in Fig. 2 (a). The other set of gratings, S3 and S4, has similar bandwidth and modulations, but with a centre Bragg wavelength of 1546 nm. The reflection spectra are shown in Fig. 2 (b). Each set of gratings was connected to one arm of the coupler. The multiplexed signal was reflected back to a photodetector module of the tuneable laser system, and was then processed by a computer. The multiplexed output signal of the four gratings is shown in Fig. 2 (c). From the figure, it can be seen that: (i) there are some high frequency ripples on the first set (λ_B = 1530 nm), which was caused by some dust on the phase mask or on the fibre during fabrication; and (ii) the two sets are partially overlapping, which in the WDM scheme, could lead to crosstalk between two the sets of gratings. Despite these issues, we demonstrate that through the DWT demodulation with BLT, they can be mitigated with minimal adverse effects on the measurements.

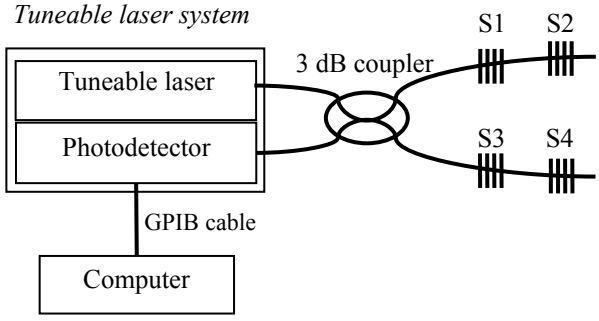

Fig. 1. Experimental setup of the sensor system.

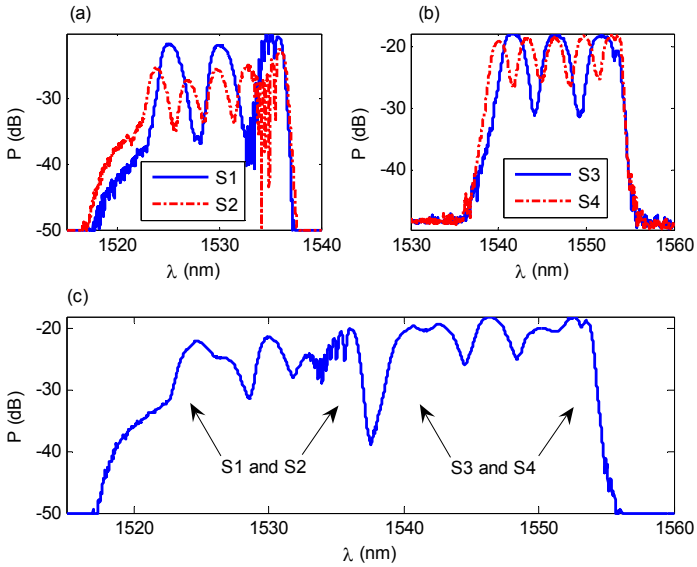

Fig. 2. Individual AMCFBGs before multiplexing: (*a*) S1 and S2, (*b*) S3 and S4; and (*c*) multiplexed signal with spectral overlapping.

3.2 Demodulation of multiplexed signal

The unique signatures, i.e., the sinusoidal modulations of the gratings, can be extracted by taking the DWT to obtain the detail coefficients. The coefficients are in the same domain as the original signal, with each level showing a particular band of frequency depending on the number of data points. For the acquired signal having 9001 points and modulation frequencies of 3 and 5 periods, the modulations of S1 and S3 appear on the 9th-level detail coefficients, while the modulations of S2 and S4 appear on the 8th-level; and these are shown in Figs. 3 (a) and 3 (b), respectively. The y-axis is the relative (mean-removed) power of the original spectrum.

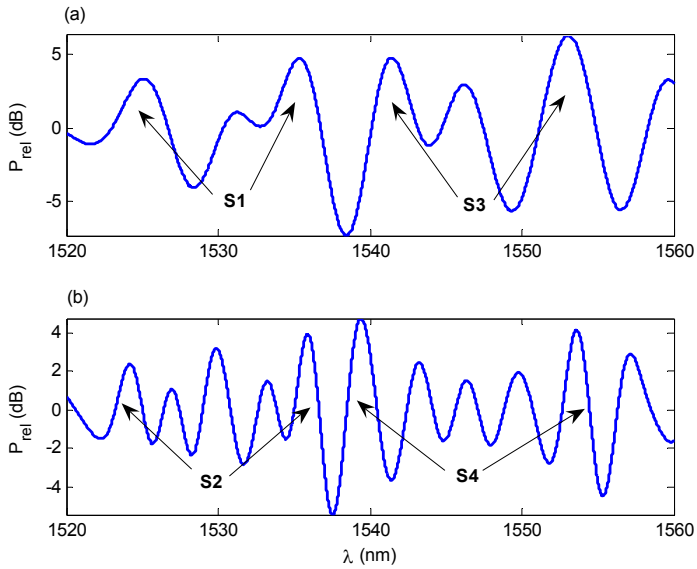

Fig. 3. (*a*) Ninth and (*b*) eighth-level detail coefficients for gratings with modulations of 3 and 5 periods, respectively.

From the figure, the sinusoidal modulations of all four gratings are distinctly identified, with the same modulation period appearing on the same wavelet level. In other words, the multiplexed signal has been successfully demultiplexed and demodulated whereby the measurand-induced wavelength shifts can be individually measured by tracking the 'phase-shifts' of the modulations. Note that the modulated signals are very smooth that are essentially unaffected by the noise and undesired ripples. This is because the ripples are of different frequencies from those of the sinusoidal modulations, and so after taking the DWT they would appear on different wavelet levels. The multiplexing of AMCFBGs can be extended by adding more overlapped gratings with different modulation periods, as well as with different centre Bragg wavelengths. The demodulated signals of the gratings having the same modulation period will be shown on the same wavelet level, and those with different periods will be shown on different wavelet levels. Regarding the resolution of the sensor system, since the tuneable laser operated at a step size of 5 pm, this corresponds to a strain resolution of ~4 με. The resolution was further increased to ~1 με after applying a cubic spline interpolation method to the modulated signals, i.e., the detail wavelet coefficients.

3.3 Strain and crosstalk measurements

The strain response and crosstalk of the two sets of partially overlapped AMCFBGs are investigated. In such a case, the crosstalk mainly comes from two sources: 'self-crosstalk' from the complete overlapping within each set of gratings having the same centre Bragg wavelength; and partial overlap between adjacent sets of gratings. With the same setup as in Fig. 1, the four gratings were suspended vertically next to each other, with plastic cups hanging at the lower ends by using cotton threads that were threaded into the splice protectors. Strains were applied to S4 by adding ten 20-cent coins (each weighs 11.3 g, which corresponds to a strain of 125 με), and also applied alternately to S2 by adding a 20-cent coin at every two 20-cent coins added to S4 (i.e., a total of five 20-cent coins were added). The other two gratings S1 and S3 were left unstrained. For each coin applied, ten readings were taken. Fig. 4 (a) shows the measured strain of S2 and S4 as a function of applied strain. The lines are the ideal strain values. It can be seen that both gratings with measured strains match very well with the applied values. For applied strains up to 1250 με, the accuracy is within ±20 με. Fig. 4 (b) shows the corresponding measured strain response of the two unstrained gratings S1 and S3, which is indeed a measure of the amount of crosstalk (and possibly system errors) due to the strained gratings. From the figure, the maximum crosstalk of S2 and S4 is about 24 με. In addition, by removing one set of overlapped gratings, and repeating the experiment (by just adding 20-cent coins to one grating while leaving the other unstrained), it is found that the maximum 'self-crosstalk' is about 16 με. Such a small amount of crosstalk implies that the undesired effects of spectral shadowing and partial overlapping have very little influence on this multiplexing technique.

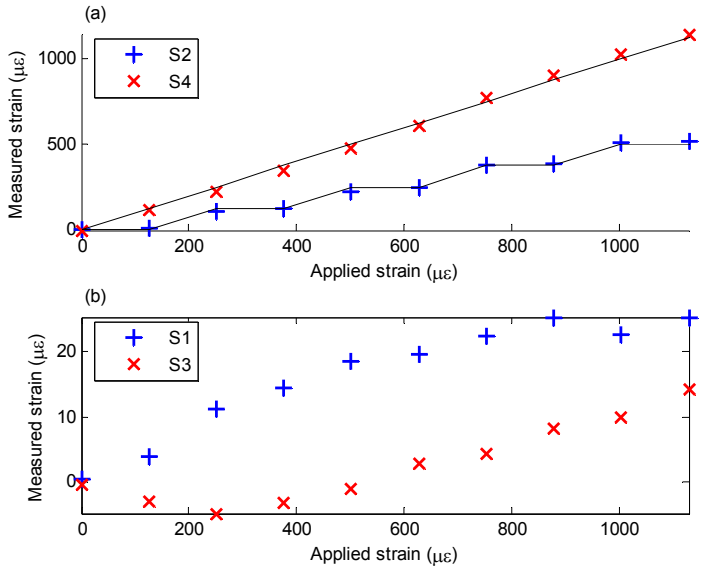

Fig. 4. Strain measurements of (*a*) gratings S2 and S4; and (*b*) unstrained gratings S1 and S3 showing the crosstalk due to S2 and S4.

4. SIMULTANEOUS TWO-PARAMETER SENSING

4.1 Simultaneous sensing

The feasibility of this multiplexing technique is demonstrated in the simultaneous measurement of strain and temperature of an aluminium (Al) alloy plate using the reference grating method [20]. The strain sensor is firmly attached to the Al-alloy plate running parallel with the direction of the strain field. The temperature sensor is placed under the same environmental conditions but is unstrained, being shielded from the strain field of the Al-alloy plate. The former experiences wavelength shifts due to both strain ($\Delta\varepsilon$) and temperature (ΔT) change, while the latter only experiences the shift due to temperature change. The set of simultaneous linear equations is correspondingly given by,

$$\begin{pmatrix} \Delta\lambda_{B1} \\ \Delta\lambda_{B2} \end{pmatrix} = \begin{pmatrix} k_{\varepsilon 1} & k_{T1} \\ 0 & k_{T2} \end{pmatrix} \begin{pmatrix} \Delta\varepsilon \\ \Delta T \end{pmatrix}, \tag{4}$$

where subscripts 1 and 2 represent strain and temperature sensors, respectively; $k_{\varepsilon 1} = (1 - p_e)\lambda_B$ where p_e is the photoelastic coefficient; $k_{T1} = [(1 - p_e)\alpha_{Al} + p_e\alpha_F + \xi_F]\lambda_B$ where α is the coefficient of thermal expansion, ξ is the thermo-optic coefficient, subscripts Al and F represent the Al-alloy plate and silica fibre, respectively; $k_{T2} = (\alpha_F + \xi_F)\lambda_B$; and λ_B is the centre Bragg wavelength. By solving the measurands-vector, the strain and temperature change are given by,

$$\Delta\varepsilon = \frac{1}{k_{\varepsilon 1}}\Delta\lambda_{B1} - \frac{k_{T1}}{k_{\varepsilon 1}k_{T2}}\Delta\lambda_{B2}; \quad \Delta T = \frac{1}{k_{T2}}\Delta\lambda_{B2}, \tag{5}$$

after expanding the equations. Note that the expression for the strain has the temperature-compensation included. The measurand-induced responses (i.e., sensitivity coefficients), can be experimentally obtained by measuring the wavelength shifts in response to the strain and temperature. Specifically, the responses $k_{\varepsilon 1}$ and k_{T2} can be measured using an unrestrained AMCFBG, whereas k_{T1} needs to be measured with a grating attached onto the Al-alloy plate because of the thermal expansion mismatch between the plate and the silica fibre.

However, in our demonstrative experiment for simultaneous sensing, since no external strain will be applied to the plate, the strain is primarily thermally-induced from the temperature change of the plate. As such, it is assumed that both sensors experience the same temperature change (of the plate), neglecting the thermal mismatch between the plate and the silica fibre. In this special case, Eq. (5) is modified to,

$$\Delta\varepsilon = \frac{1}{k_\varepsilon}(\Delta\lambda_{B1} - \Delta\lambda_{B2}); \quad \Delta T = \frac{1}{k_T}\Delta\lambda_{B2}, \tag{6}$$

where the Bragg wavelength shift, strain and temperature change are represented in units of pm, με and °C, respectively. The strain response k_ε is obtained as before, and the temperature response k_T is obtained from the grating attached onto the plate. The strain obtained from Eq. (6) is effectively called the thermal strain.

4.2 Sensor characterisation

From Eq. (6), the strain response was measured by applying 10-cent coins to a grating that was vertically suspended with a container attached at the lower end. The corresponding strain for one 10-cent coin (with a weight of 5.65 g) is 63 με. The temperature response was measured by putting a grating that was attached onto the plate into a bath of hot water and measuring the temperature change (46 °C – 79 °C) using a thermocouple. Figs. 5 (a) and 5 (b) show the strain and temperature responses of an AMCFBG with a centre Bragg wavelength of 1568 nm, respectively.

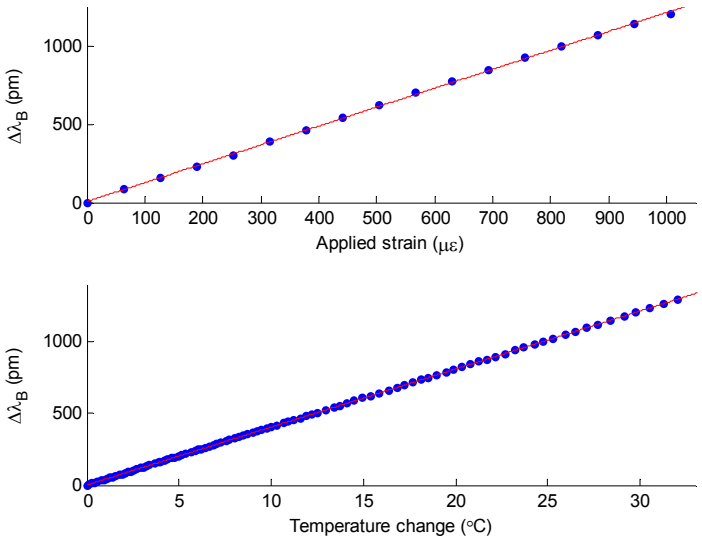

Fig. 5. (a) Strain and (b) temperature responses of an AMCFBG. Temperature response was measured with the grating attached onto the Al-alloy plate.

The figures are plotted from the 'phase-shift' of the centre Bragg wavelength as a function of the change in the measurands. The lines are the linear-regression fits of the measured data points. Based on the slope of the linear regression fit, the strain and temperature sensitivity coefficients are 1.20 pm/με and 38.12 pm/°C, respectively.

4.3 Simultaneous measurement of strain and temperature of an aluminium-alloy plate

According to the reference grating method, to simultaneously measure the strain and temperature change of the Al-alloy plate, one of the AMCFBG sensors was adhered firmly onto the plate with epoxy resin, whereas the other sensor was loosely attached such that it was free and unstrained from any strain field of the plate. The plate was placed inside a polyurethane foam box to minimise possible environmental perturbations. The sensors were left for about 10 min in order for the adhesive to dry. After that, measurements of the wavelength shifts of the sensors using the tuneable laser system were made for a period of 18 h. By using Eq. (6), the strain and temperature change are shown in Fig. 6. From the figure, both the strain and temperature curves changed in a much correlated manner, due to the fact that the strain is mostly thermally-induced. The results are expected as there was no external strain applied throughout the experiment. The net change in strain and temperature during this 18 h period were about 40 με and 1.5 °C, respectively. Since the plate was placed inside a foam box that had a relatively high heat capacity, the change in temperature was a bit small. By plotting a graph of temperature vs. strain, the slope of the linear regression fit gives a thermal strain sensitivity of 33 με/°C. The small and local fluctuations are mainly from ambient environmental perturbations, especially from human and wind movements.

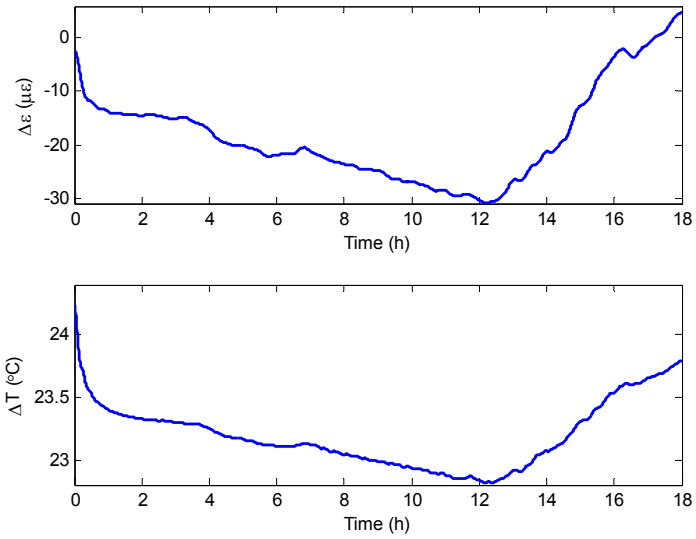

Fig. 6. Simultaneous measurement of strain and temperature of an Al-alloy plate.

5. CONCLUSIONS

A spectral-overlap multiplexing technique has been presented and experimentally demonstrated using AMCFBGs with the same spectral characteristics. The DWT was used for demultiplexing and demodulation, and the BLT denoising technique was incorporated with it to reduce the noise of the multiplexed signal. Experimental results showed that the absolute error is within ±20 με; the "self-crosstalk" of the overlapped gratings and the crosstalk between adjacent sets of overlapped gratings are 16 με and 24 με, respectively. Using the tuneable laser system with an interpolation method, the resolution of the multiplexed system is 1 με. This multiplexing technique was successfully applied to the simultaneous measurement of strain and temperature of an Al-alloy plate. By employing this multiplexing technique, the number of gratings to be multiplexed in conjunction with the WDM can be increased by several times, and this would be beneficial to applications where a large number of gratings are required.

ACKNOWLEDGEMENTS

This research was supported by the Australian Research Council and the Roads and Traffic Authority, under the Linkage Projects funding scheme (project number LP0347804).

REFERENCES

[1] A. Othonos and K. Kall, *Fiber Bragg Gratings*, Artech House, Boston (1999)
[2] R.M. Measures, *Structural Monitoring with Fiber Optic Technology*, Academic Press, San Diego (2001)
[3] J.M. Lopez-Higuera (ed), *Handbook of Optical Fibre Sensing Technology*, Wiley, Chichester (2002)
[4] F.T.S. Yu and S. Yin (eds), *Fiber Optic Sensors*, Marcel Dekker, New York (2002)
[5] Y.J. Rao, "In-fibre Bragg grating sensors", Meas. Sci. Technol. **8**, 355-375 (1997)
[6] S. Huang, M.M. Ohn, M. LeBlanc, R. Lee and R.M. Measures, "Fiber optic intra-grating distributed strain sensor", Proc. SPIE **2294,** 81-92 (1994)
[7] M. Volanthen, H. Geiger and J.P. Dakin, "Distributed grating sensors using low-coherence reflectometry", J. Lightwave Technol. **15,** 2076-2082 (1997)
[8] A.M. Gillooly, K.E. Chisholm, L. Zhang and I. Bennion I, "Chirped fibre Bragg grating optical wear sensor", Meas. Sci. Technol. **15,** 885-888 (2004)
[9] Y. Okabe Y, R. Tsuji and N. Takeda, "Application of chirped fiber Bragg grating sensors for identification of crack locations in composites", Composites: Part A **35,** 59-65 (2003)

[10] P.C. Won, J. Leng, Y. Lai and J.A.R. Williams, "Distributed temperature sensing using a chirped fibre Bragg grating", Meas. Sci. Technol. **15,** 1501-1505 (2004)
[11] A. Nand, D.J. Kitcher, S.A. Wade, T.B. Nguyen, G.W. Baster, R. Jones and S.F. Collins, "Determination of the position of a localized heat source within a chirped fibre Bragg grating using a Fourier transform technique", Meas. Sci. Technol. **17,** 1436-1445 (2006)
[12] P. Childs, "An FBG sensing system utilizing both WDM and a novel harmonic division scheme", J. Lightwave Technol. **23,** 348-354 (2005)
[13] P. Childs P and G.D. Peng, "Simultaneous detection of 8 spectrally overlapping carrier modulated fibre Bragg gratings", Electron. Lett. **42,** 274-276 (2006)
[14] J.M. Seo, S.H. Kim, I.B. Kwon, J.J. Lee and D.J. Yoon, "Intensity-modulated multiplexing of fiber Bragg grating sensors", Smart Mater. Struct. **14,** 177-182 (2005)
[15] K. Hotate, M. Enyama, S. Yamashita and Y. Nasu, "A multiplexing technique for fibre Bragg grating sensors with the same reflection wavelength by the synthesis of optical coherence function", Meas. Sci. Technol. **15,** 148-153 (2004)
[16] C.Z. Shi, C.C. Chan, W. Jin, Y.B. Liao, Y. Zhou and M.S. Demokan, "Improving the performance of a FBG sensor network using a genetic algorithm", Sens. Actuators A **107,** 57-61 (2003)
[17] J.M. Gong, J.M.K. MacAlpine, C.C. Chan, W. Jin, M. Zhang and Y.B. Liao, "A novel wavelength detection technique for fiber Bragg grating sensors", IEEE Photon. Technol. Lett. **14,** 678-680 (2002)
[18] Y.J. Rao, Z.L. Ran and C.X. Zhou, "Fiber-optic Fabry-Perot sensors based on a combination of spatial-frequency division multiplexing and wavelength division multiplexing formed by chirped fiber Brag grating pairs", Appl. Opt. **45,** 5815-5818 (2006)
[19] A.C.L. Wong, P.A. Childs and G.D. Peng, "Multiplexed fibre Fizeau interferometer and fibre Bragg grating sensor system for simultaneous measurement of quasi-static strain and temperature using discrete wavelet transform", Meas. Sci. Technol. **17,** 384-392 (2006)
[20] M.G. Xu, H. Geiger and J.P. Dakin, "Modeling and performance analysis of a fiber Bragg grating interrogation system using an acousto-optic tunable filter", J. Lightwave Technol. **14,** 391-396 (1996)